

Structural Evolution in Isothermal Crystallization Process of Poly(L-lactic acid) Enhanced by Silk Fibroin Nano-Disc

Amit Kumar PANDEY¹, Vimal KATIYAR², Hideaki TAKAGI³, Nobutaka SHIMIZU³,
Noriyuki IGARASHI³, Sono SASAKI¹ and Shinichi SAKURAI^{1,*}

¹Department of Biobased Materials Science, Kyoto Institute of Technology, Matsugasaki, Kyoto,
606-8585, Japan

²Department of Chemical Engineering, Indian Institute of Technology Guwahati,
Guwahati, Assam 781039, India

³Photon Factory, Institute of Materials Structure Science,
High Energy Research Organization, 1-1 Oho, Tsukuba, 305-0801, Japan

1 Introduction

The nucleating effect of silk fibroin nano-disc (SFN) on the crystallization behavior of poly(L-lactic acid) (PLLA) was investigated by simultaneous synchrotron small- and wide-angle X-ray scattering measurements. For the isothermal crystallization at 110 °C from the melt, the induction period of the PLLA specimens containing 1% SFN was reduced compared to that of the neat specimens, indicating the acceleration of the nucleation of PLLA. The final degree of crystallinity was also increased, and the crystallization half-time was decreased, which indicates that the overall crystallization process was accelerated. Furthermore, the final value of the crystallite size (the lateral size of the crystalline lamella) was slightly lower for the specimens containing 1% SFN than that for the PLLA neat specimen, although the crystallites started growing much earlier. However, it was found that there was no effect of SFN on the growth rate of the crystallite size. The lamellar thickening process was also accelerated with a clear overshooting phenomenon with the inclusion of 1% SFN. As for the polymorphism, the α' phase is dominant with about 96%, but a small amount of the phase (4%) is found to exist. It was found that the SFN can also accelerate the formation of the minor α phase as well as the major α' phase.

2 Experimental

The PLLA samples used in this study are obtained from NatureWorks LLC. As shown in Table 1, one of them bears 1.4% D content (PLLA4032D) and the other 0.5% D content (PLLA2500HP), which enabled us to study the effects of the optical impurity on the crystallization of PLLA with or without the presence of SFN. The SFN is a nanoparticle that was extracted from wastes of the muga silk (*Antheraea assama*) cocoon. The crystalline portion (the sheets) of the silk fibroin was isolated by using the acid-hydrolysis method. The obtained extract comprises 83.8% L-alanine, and the well-defined disc-like nanoparticles were obtained with the average diameter and thickness of ~45 nm and ~3 nm, respectively. The composites of PLLA and SFN were prepared by the solution-casting method by using dichloromethane as a solvent. The specimens are labeled as D1.4/SFN(x) or

Table 1: Sample characteristics

Sample	Code name	D content	M_n (GPC)	M_w (GPC)	M_w/M_n (GPC)
PLLA2500HP	D0.5	0.5%	1.74×10^5	3.86×10^5	2.22
PLLA4032D	D1.4	1.4%	1.66×10^5	3.40×10^5	2.05

D0.5/SFN(x), where the numbers after D denote the % of D moiety in PLLA, and x stands for % of SFN inclusion.

The time-resolved SWAXS (small- and wide-angle X-ray scattering) measurements were carried out by using the synchrotron radiation as an X-ray source at the beamline BL-6A of Photon Factory at the KEK (High-Energy Accelerator Research Organization) in Tsukuba, Japan. The wavelength of the incident X-ray beam was 0.150 nm. The sample was packed into an aluminum cell, which had a diameter of 4 mm and thickness of 1 mm. The specimens were sandwiched by a couple of pieces of the polyimide (Kapton) film, obtained from DuPont-Toray Co., Ltd., Tokyo, Japan. Firstly, the specimens were melted at 200 °C for approximately 5 min, and then the sample cell was quickly moved to another heater block, which was maintained at 110 °C, and then the simultaneous SWAXS measurement was performed. Note here that this isothermal crystallization temperature (110 °C) can be considered to be located in regime III. This is because Song et al. (2018) have reported that PLLA specimens with 100% and 98% L moieties show the regime II at higher temperature and regime III at lower temperature with the transition temperature of 120 °C [1]. The actual sample temperature was monitored by a temperature sensor, which was directly attached to the sample. The stabilization time for the temperature equilibration after the T-jump was 15s and the temperature fluctuation was less than 0.3 °C. The scattering vector q was calibrated by using collagen for SAXS (small-angle X-ray scattering) and polyethylene for WAXS (wide-angle X-ray scattering). The SAXS and WAXS patterns were recorded at every 5 s with the X-ray exposure time of 5s. The background scattering was subtracted. The one-dimensional SAXS and WAXS profiles were obtained by taking the circular average of the 2d-SAXS pattern and the sector average of the 2d-WAXS pattern, respectively.

3 Results and Discussion

The changes in the WAXS profiles were measured in the isothermal crystallization process at 110 °C from the melt (200 °C). Figure 1 shows the WAXS profiles for the D1.4 neat and D1.4/SFN(1.0) specimens as a function of time. Here, q denotes the magnitude of the scattering vector, as defined by $q = (4\pi/\lambda) \sin(\theta/2)$, with λ and θ being the wavelength of X-ray and the scattering angle, respectively. As shown in Figure 1, in the early stage, there is no crystalline peak, which shows the presence of 100% amorphous phase. As time goes on, a crystalline peak appears (which has been shown by the red arrow in Figure 1). The induction period (t_0) of the crystallization is evaluated from the first detection of the crystalline peak. It can be seen from Figure 1 that the loading 1% SFN caused the reduction of the induction period from 90s to 40s, which shows the enhancement of the crystallizability by SFN. The time evolution of the degree of crystallinity was calculated from the WAXS profiles. The peak decomposition was conducted, and the degree of crystallinity (ϕ_{WAXS}) was evaluated. The calculated ϕ_{WAXS} plotted as a function of time in Figure 2. As can be seen from Figure 2, the final degree of the crystallinity has been increased by the inclusion of 1% SFN. Judging from the slope of the curve at $t = t_{0.5}$ (where $t_{0.5}$ is the crystallization half-time at the 50% of the final crystallinity attained) in Figure 2, it can be considered that the crystallizability of PLLA is increased by adding 1% SFN. The induction period, the final degree of crystallinity and the crystallization half-time of all the specimens were calculated from the results of Figure 2. It is clearly observed that $t_{0.5}$ is decreased by loading of SFN, indicating the acceleration of the crystallization rate. Furthermore, it is important to check the effect of SFN on the formation of the crystal polymorph (α and α' phases). For this purpose, the evaluation of the fraction of α and α' phases formed during the isothermal crystallization at 110 °C was conducted by analyzing the (200)/(110) reflection. Since there observed a small shoulder around $q = 12.2 \text{ nm}^{-1}$, we tried to decompose the shoulder peak (α phase) from the main peak (α' phase). Figure 3 shows an example of the peak decomposition in the range of $11 < q < 13 \text{ nm}^{-1}$, ensuring the perfect peak decomposition.

Figure 4 shows the changes in the Lorentz-corrected SAXS profiles as a function of time for the D1.4 neat and D1.4/SFN(1.0) specimens. Here, the scattering intensity, $I(q)$, is corrected as $q^2 I(q)$ by multiplying q^2 . In the early stage of the crystallization, there was no observation of the peak. At $t = 180 \text{ s}$ for the D1.4 neat or $t = 90 \text{ s}$ for the D1.4/SFN(1.0) specimen, a clear scattering peak was observed, which indicates the development of the lamellar stacking with sandwiching the amorphous layers. It is notable to observe that the WAXS peak appears earlier than the SAXS peak (Figures 1 and 4). Such a result indicates that during the early stage of crystallization, the lamellar stacks are incomplete by noting $t_0 = 90 \text{ s}$ and 40 s for the D1.4 neat and D1.4/SFN(1.0) specimens (see Figure 1). In other words,

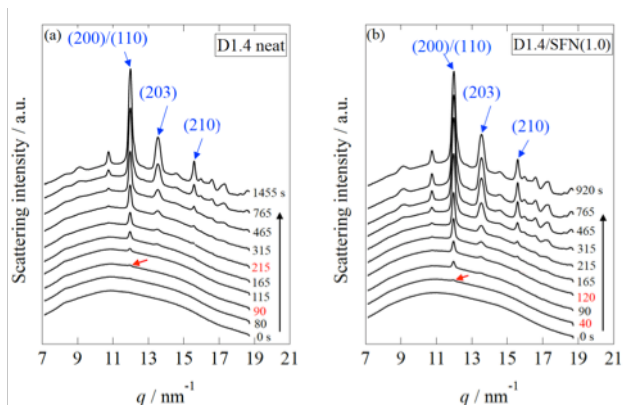


Fig. 1 Time-resolved WAXS profiles of (a) D1.4 neat (b) D1.4/SFN(1.0) specimens. The red arrow indicates the first detection of the peak.

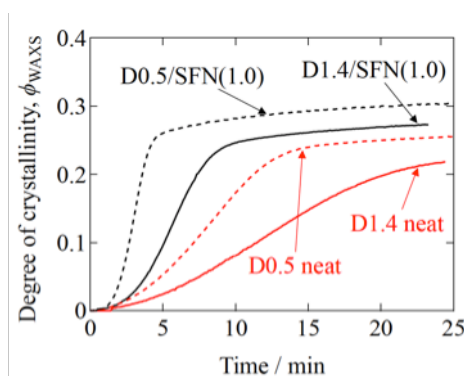


Fig. 2 Degree of crystallinity as a function of time for the isothermal crystallization at 110 °C.

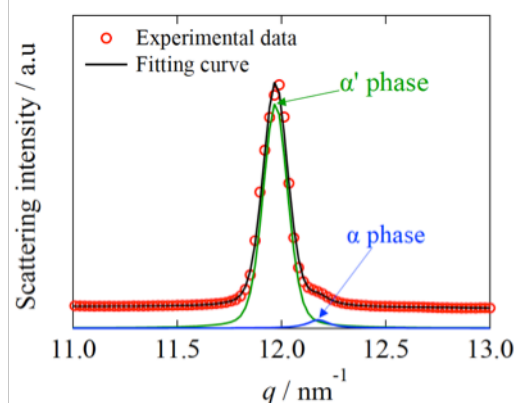


Fig. 3 Decomposition of the (200)/(110) reflection peak in the range of $11 < q < 13 \text{ nm}^{-1}$.

single lamellae (without stacking) are generated in the early stage of the crystallization.

The intensity of the peak observed at $q = 0.29 \text{ nm}^{-1}$ increases as a function of time. From the peak position (q^*), the long period (D) of the lamellar stacks was evaluated as $D = 2\pi/q^*$. As seen in Figure 4, the SAXS peak moves towards the higher q as the crystallization proceeds. Increase in q suggests the decrease in D . As shown in Figure 5a, the repeating distance of the lamellar stacks (D) decreases as a function of the crystallization time. This result seemed to be opposed to the process of

crystallization. In order to understand this behavior, we evaluated the average thickness of the crystalline lamella (L). To evaluate L , the correlation function $\gamma(r)$ was calculated from the 1d-SAXS profile through the following equation (inverse Fourier transform method):

$$\gamma(r) = \frac{\int_0^\infty I(q)q^2 \cos(qr) dq}{\int_0^\infty I(q)q^2 dq}$$

Here, $\gamma(r)$ is the correlation function and r is the distance in the real space. Figure 5 shows thus-evaluated L and D and the ratio (L/D) as a function of time during the isothermal crystallization upon T-jump from 200 °C to 110 °C. As a result (Figure 5b), the average lamellar thickness increases with time, which is reasonable as a crystallization behavior. Therefore, the decreasing behavior of D is also reasonable, as schematically shown in Figure 6. Upon crystallization, shrinkage takes place. Since the lamella thickens with time, this results in the decrease of D (Figure 6b,c), as an amorphous layer thickness is decreased to a greater extent as compared to the increasing extent of L (lamellar thickness).

It should be noted here that the average lamellar thickness (L) did not monotonically increase as a function of time, as the increasing tendency turns over around 7 min for the D0.5 neat specimen or 4 min for the D0.5/SFN(1.0) specimen. The reason why L decreased a bit before reaching a constant value may be explained by the formation of new lamellae. It may be explained that in prior to 7 min for the D0.5 specimen or 4 min for the D0.5/SFN(1.0) specimen, a new thin lamellae may be formed from the amorphous region. This argument has been recently reported by our group [2,3] for the isothermal crystallization of the D0.5 specimen in the

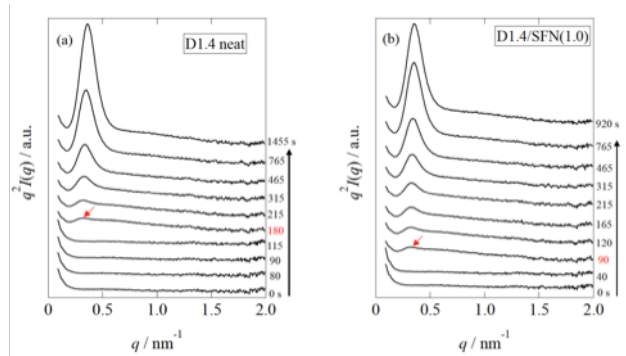


Fig. 4 Changes in the Lorentz-corrected SAXS profiles as a function of time for (a) D1.4 neat and (b) D1.4/SFN(1.0) specimens during the isothermal crystallization at 110 °C from melt. The red arrow indicates the first detection of the peak.

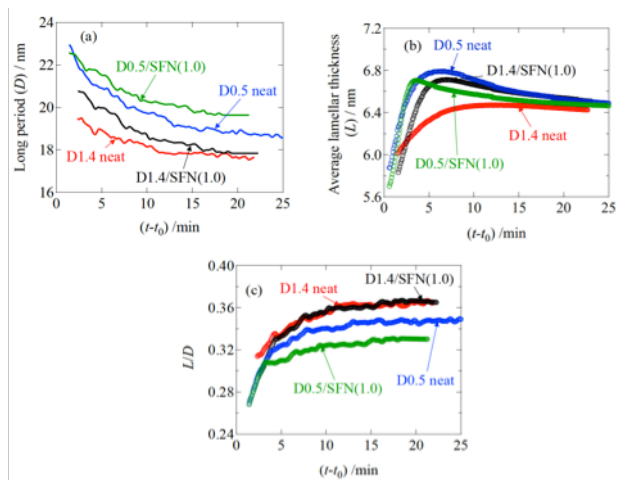


Fig. 5 (a) Long period (D), (b) average lamellar thickness (L), and (c) L/D as a function of $(t - t_0)$, where t_0 is the induction period.

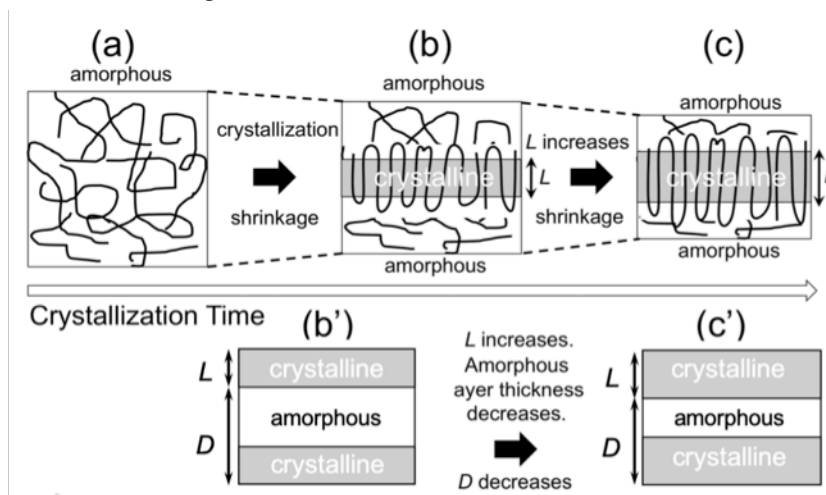


Fig. 6 Schematic illustrations showing the change in the nanostructure upon crystallization of PLLA (a) at the amorphous state before crystallization of the polymer melt and (b) in an early stage of crystallization. (c) Lamellar thickening in the subsequent stage of the crystallization. Note that the illustrations are focusing on the change in the long period (D) of the lamellar stacks. (b') and (c') correspond to the states of (b) and (c), respectively. The illustrations of (b') and (c') are intended to explain the reason why D decreases as a function of time along the proceeding of crystallization, where L increases with time [3,4].

presence of a special plasticizer (OMG) at 100 °C from the melt, where a higher order peak was observed in the Lorentz-corrected SAXS profiles. Furthermore, as shown in Figure 5b, the initial average thickness of the lamella is thinner for the case of 1% addition of SFN as compared to the neat specimen. This result may explain the mechanism of acceleration of the crystallization by SFN to lower the activation energy of the crystallization with lowering of the thickness of the critical nucleus [3]. Note here that $L = 6.3$ nm is the maximum available for the D1.4 sample because of the D moiety (optical impurity), which is distributed with every 70 repeating units of L moieties when the homogeneous distribution of the D moieties in the main chain of PLLA is assumed. Therefore, the final value of L for the D1.4 specimens is somewhat larger. This would imply the random distribution of the D moieties in the main chain of PLLA, further meaning that the Gaussian distribution of the L unit repeating length gives its larger value as compared to the average value which results in $L = 6.3$ nm.

The ratio L/D seems to be the crystallinity in the stacks of the lamella. To check the increasing tendency of this ratio as a function of time during the isothermal crystallization, L/D is plotted as a function of time in Figure 5c. It is then found that the monotonic increase in L/D is then leveled off without the overshooting, as is seen in the plot of L in Figure 5b. Moreover, there is observed no effect of the SFN. This is very much contrasted with the crystallization behavior shown in Figure 2. As shown in Figure 5c, L/D is larger than ϕ_{WAXS} (Figure 2). The reason why L/D is larger than ϕ_{WAXS} is because the lamellar stacks are sparsely dispersed in the matrix of polymer melts, and they do not completely fill the specimen space in the early stage. Then, the lamellar stacks completely fill the space in the specimen in the late stage, where the L/D is almost identical to ϕ_{WAXS} . It is noteworthy that there is no effect of SFN on the behavior of L/D as shown in Figure 5c for the D1.4 neat and D1.4/SFN(1.0) specimens. At this moment, it is unclear that this result is universal, irrespective of the amount of loading. More detailed study is required. As for the D0.5 neat and D0.5/SFN(1.0) specimens, the SFN even reduces the L/D value, which is opposed to the overall behavior shown in Figure 2. This result may suggest that the SFN enhances the formation of the isolated lamellae without stacking.

4 Conclusion

The crystallization behavior of the neat PLLA and PLLA/SFN(1.0) specimens was investigated by using the time-resolved SWAXS techniques. The results showed that the loading SFN shortens the induction period and the increase in the ultimate degree of crystallinity. The crystallization half-time was reduced, which suggests that the overall crystallization process was accelerated. Furthermore, the crystallite size was very slightly reduced, but the growth rate of the crystallites was unchanged. The amount of the α' and α phases were increased as a function of time, while the fraction was constant (only about 4% of α phase). The SAXS results suggest that the lamellar thickening process was accelerated, and the thickness of the initial lamella was decreased by loading 1% SFN in PLLA. This result clearly indicates that the thickness of the critical nucleus is reduced by the SFN.

References

- [1] Song, P.; Sang, L.; Jin, C.; Wei, Z., *Polymer*, **134**, 163 (2018).
- [2] P. T. N. Diep, H. Takagi, N. Shimizu, N. Igarashi, S. Sasaki, S. Sakurai, *J. Fiber Sci. Technol.*, **75**, 99 (2019).
- [3] A. K. Pandey, P. T. N. Diep, R. Patwa, V. Katiyar, S. Sasaki, S. Sakurai, in *Advances in Sustainable Polymers - Synthesis, Fabrication and Characterization* (Editors: V. Katiyar, A. Kumar, N. Mulchandani), Springer Nature Singapore, Chapter 14 (2019). DOI: 10.1007/978-981-15-1251-3
- [4] A. K. Pandey, V. Katiyar, H. Takagi, N. Shimizu, N. Igarashi, S. Sasaki, S. Sakurai, *Materials*, **12**, 1872 (2019).

Research Achievements

1. Amit Kumar Pandey, Best Oral English Presentation Awards of the Society of Rubber Science and Technology, Japan (2019).

* shin@kit.ac.jp